Tu_R04_11

Elastic Parameters Estimation Using Reservoir-Oriented Joint Migration Inversion for Norwegian Sea Field Data

A. Garg[1]*, H. Masoomzadeh[2], S. Baldock[2], D.J. Verschuur[1]

[1] Delft University of Technology; [2] TGS

Summary

We present the first field data application of the full reservoir-oriented joint migration inversion (JMI-res) workflow to estimate the reservoir elastic parameters. JMI-res first reconstructs the fully redatumed data (local impulse responses) at the target reservoir level, while correctly accounting for interbed multiples and transmission losses from the overburden and then applies a localised FWI on the estimated impulse responses to get the reservoir elastic parameters. With this approach, we avoid the need to apply a full elastic process for the whole subsurface. In this paper, we show that JMI-res provides reliable local target impulse responses, thus yielding high-resolution elastic parameters, compared to a standard redatuming process based on time reversal, courtesy of proper handling of interbed multiples and transmission losses in the redatuming step. Even for cases where there are no clear interbed multiples cross-cutting the reservoir, the improvement can be substantial due to recovered transmission losses in the overburden.

Introduction

Both seismic migration (Bednar, 2005) and full waveform inversion (elastic-FWI) (Virieux and Operto, 2009) aim to delineate the prospective reservoir. Seismic migration does it by creating the subsurface reflectivity image whereas elastic-FWI does this by directly estimating actual subsurface elastic parameter models. As actual elastic parameters can be linked to reservoir properties (e.g. porosity and lithology), angle-dependent migration images in the reservoir area are also used to estimate elastic parameters (Russell, 2014). However, both migration and FWI approaches have their limitations. Most seismic migration methods fail to account for interbed multiples and transmission losses. As a result, in a complex subsurface scenario, the reservoir image contains the spurious events related to overburden complexities, which ultimately affects the elastic parameters estimation. On the other hand, even though elastic-FWI accounts for all multiple energy, it is still avoided in the full bandwidth due to the associated computational costs. Instead, acoustic or pseudo-acoustic FWI methods (Hobro et al., 2014) are used, even for P-mode elastic data, that fail to explain the true elastic amplitudes and possibly give incorrect elastic parameters.

To overcome the above mentioned issues, Garg and Verschuur (2018) proposed the reservoir-oriented joint migration inversion (JMI-*res*) (fig. 1a) to estimate the elastic parameters from the surface seismic data. JMI-*res* first reconstructs the data at the reservoir level (local impulse responses **X**) that would have been recorded if both sources and receivers were at the reservoir level within the subsurface. This procedure is commonly called as redatuming (Beryhill, 1984; Schuster and Zhou, 2006). However, unlike most redatuming appoaches, JMI-*res* ensures that multiple scattering and transmission losses are correctly explained in this redatuming step. This is apart from the velocity estimation being an integral part of JMI-*res* and the fact that the true elastic P-P reflection characteristics are preserved without explicitly using the full elastic wave equation (Garg and Verschuur, 2017). Then, elastic-FWI is applied only for the local impulse responses in the target-area to estimate the reservoir elastic parameter models. Thus avoiding the need to apply a full elastic approach for the whole subsurface.

Here, we present the first application of JMI-*res* on a field dataset by using a 2D marine data line from the Norwegian Sea. We will show the results at each step in JMI-res and finally compare the estimated elastic parameters with the well-log measurements. Also, to show the influence of properly explaining the interbed multiples and transmission losses, we will also estimate the impulse responses via standard redatuming based on time reversal of seismic data and estimate the elastic parameters (fig. 1b). By comparing the elastic parameters estimated in both approaches, we will show the higher resolution that we get via JMI-*res*.

Theoretical aspects

The full JMI-*res* process, as shown in fig. 1a, can be subdivided into three substeps:

1. In the first step, we estimate the up-/downgoing elastic wavefields at the reservoir depth, via Joint Migration Inversion (JMI) (Berkhout, 2014b; Staal, 2015), while correctly explaining the scattering and transmission effects.

2. Next, the redatumed wavefields are transformed into local impulse responses (**X**) via so-called proximity transformation (Garg and Verschuur, 2016), which is a sparsity-constrained multi-dimensional deconvolution process. These local impulse responses are the data with both virtual sources and receivers at the top of reservoir.

3. Finally, the obtained **X** are used for local, target-oriented full waveform inversion (FWI-res) (Gisolf and van der Berg, 2012) to estimate the elastic reservoir parameters.

Joint Migration Inversion (JMI) (fig. 1c), as described by Berkhout (2014b) and Staal (2015), is a full-waveform type data-fitting inversion process that estimates both reflectivity image and propagation velocity model, while also estimating the up- and downgoing wavefields at all subsurface depths. The main strength of JMI lies in its forward modeling engine, called Full Wavefield Modeling (FWMod) (Berkhout, 2014a) that models all orders of scattering (primaries + internal multiples) and transmission

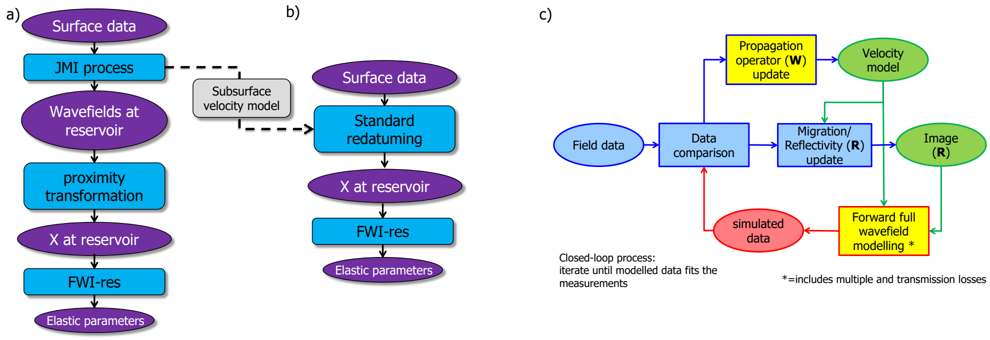

Figure 1: *Flowcharts depicting a) JMI-res, b) standard redatuming route and c) JMI.*

effects. Moreover, as shown by Garg and Verschuur (2017), JMI has the ability to explain the elastic nature of the input P-P reflection data, without explicitly imposing the full elastic wave equation. Thus, avoiding the need to go 'full elastic' for the whole subsurface in case of only P-P reflection data.

The estimated wavefields in JMI are used to get the local impulse responses (**X**) at the top of reservoir. They act as the input for FWI-*res* (Gisolf and van der Berg, 2012), which is the localised target-oriented inversion scheme. It is a wave-equation based inversion approach implemented in the linear Radon domain. Moreover, it is 1.5D in nature i.e. the inversion is carried out for each shot/CMP location at the reservoir level. In FWI-res, we invert for local elastic parameters κ (inverse of bulk modulus), M (inverse of shear modulus) and ρ (density) for the given background models that are taken from the well-log measurements. These parameters are related to P-wave (V_p) and S-wave (V_s) as follows:

$$\kappa = \frac{1}{\rho(V_p{}^2 - {}^4/_3 V_s{}^2)}, M = \frac{1}{\rho V_s{}^2}. \tag{1}$$

Field Data Example

The field data for this example is taken from 2D streamer data acquired in the Norwegian Sea. We consider a subsection of $6km$, transformed to a fixed-spread geometry with a shot and receiver spacing of $100m$ and $25m$, respectively. Fig. 2 shows the input data after some initial processing and surface-related multiple removal. From the previously done seismic procesing, we know that the events between $2.5-3s$ and around $3s$ correspond to highly attenuating layers (both elastic and anelastic) and the reservoir, respectively. Note, the data available to us also had some multiple attenuation done previously. Thus, we don't see strong internal multiples. However, we will see even now the scattering and transmission losses are strong enough to affect the reservoir elastic parameters estimation if they are not accounted for. We also account for inelastic attenuation using the effective Q (seismic quality factor) model in the propagation operator. However, the discussion on its implementation is beyond the scope of this abstract. The source wavelet is estimated from the sea-bottom reflector whereas initial $V_p(z)$ is the depth converted $V_{rms}(t)$ used in the previous time procesing.

Fig. 2b and fig. 3a show the estimated velocity model and structural reflectivity image in JMI, respectively. In order to Q.C. the estimated velocity model, we generate the image angle gathers (fig. 2c) for the estimated velocity model. We see that we are able to flatten most of the events. However, in the deeper section, we see a slighty curvy event (indicated by the arrows) in all gathers. This could possibly be due to the 3D effects that cannot be accounted for in a 2D implementation. At the same time, to see the influence of correctly explaining the scattering and transmission losses in JMI, we also generate a structural reflectivity image (fig. 3b) using primary wavefield imaging (PWM) (Davydenko and Verschuur, 2017) that does not account for former mentioned losses. We see substantial transmission losses in the deeper section around the possible reservoir area in fig. 3b in comparison to fig. 3a. The reflectors in the JMI case are much more sharp and coherently imaged, whereas they are weak and in some areas not imaged in PWM case. This comparison also indicates that we could expect similar effects later on for the estimated elastic parameters via JMI-*res* and via the standard redatuming case.

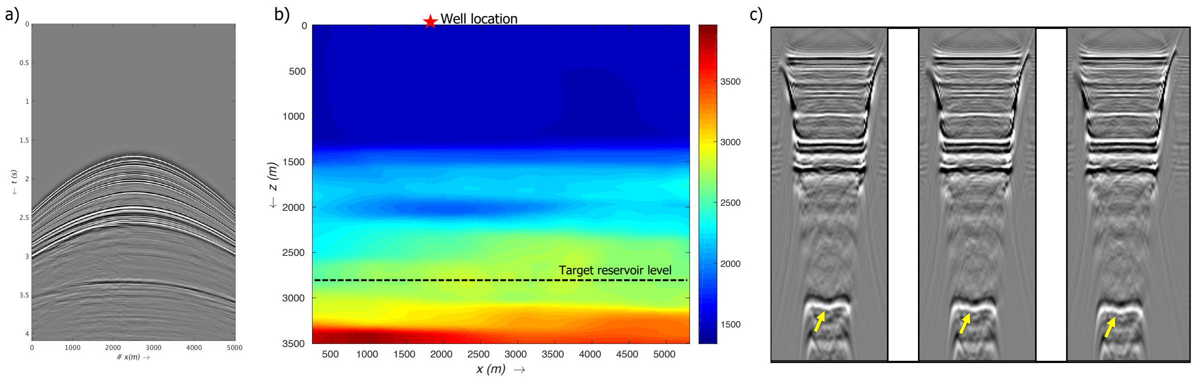

Figure 2: *a) The input shot record. b) JMI estimated velocity model. c) Image angle gathers for the JMI estimated velocity model.*

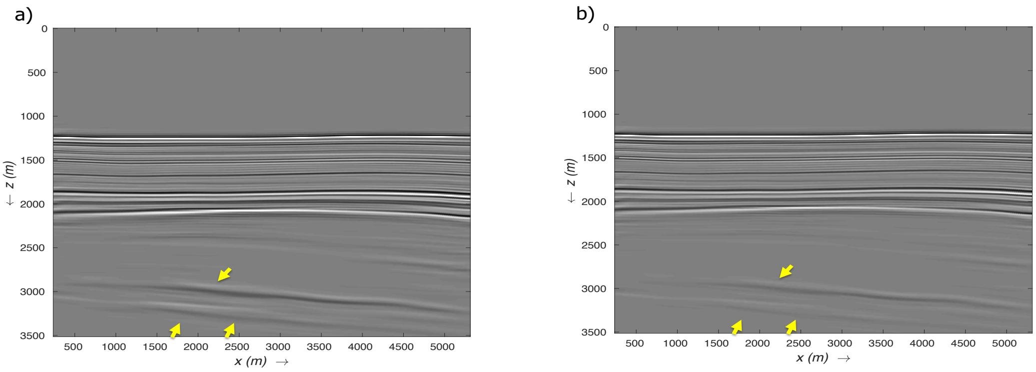

Figure 3: *Estimated structural image a) via JMI and b) via PWM, respectively. Both the images are on the same colour scale and yellow arrows indicate the major differences.*

Fig. 4a shows the comparison of estimated local impulse response (**X**) in the JMI-*res* case at the well location with the synthetic impulse response generated using well measurements. We see a reasonable match between them that shows the accuracy of the estimated **X** in the JMI-*res* case. Finally, we apply FWI-*res* to these impulse responses at the reservoir level after callibrating them with the well-log, both for JMI-*res* and the standard redatuming case, to estimate the elastic parameters (fig. 4b and 4c). Note, we only invert for κ and M as stable ρ inversion requires high-plane wave angles and P-S impulse responses too. Here, we only show the κ_{est} values, κ being the inverse of the bulk modulus, as this is a better indicator for fluid contacts in the reservoir area. In fig. 4b, we see quite a reasonable match between the estimated κ values and the well-log measured κ values for both the cases. The JMI-*res* estimated values seem to have a better fit in the deeper part. If we apply FWI-*res* to the estimated **X** for locations around the well log and plot the κ_{est} side by side and get a 2D section of estimated values (fig. 4c), we see a substantial difference between the κ_{est} values for the JMI-res and the standard redatuming case. The κ_{est} in the JMI-res case has much better coherency and resolution with sharp distinct layer boundaries in comparison to the standard redatuming case, where the κ_{est} seems more smeared. Morever, in the standard redatuming case we are not able to get any layer boundary demarcation below 3200m. This behaviour is similar to what we saw in the reflectivity image (fig. 3b) for the PWM case.

Conclusions

We presented the full JMI-*res* workflow applied to a 2D marine field data set. We showed that JMI-*res* has the potential to provide higher-resolution local impulse responses and, consequently, better estimates of the reservoir elastic parameters due to proper accounting of interbed multiples and transmission losses in the redatuming step. This is unlike the used standard redatuming case or most migration methods. Even in cases where there are no clear interbed multiples cross-cutting the reservoir, like is the case in the present example, the enhancement both in the reflectivity image and the estimated elastic parameters

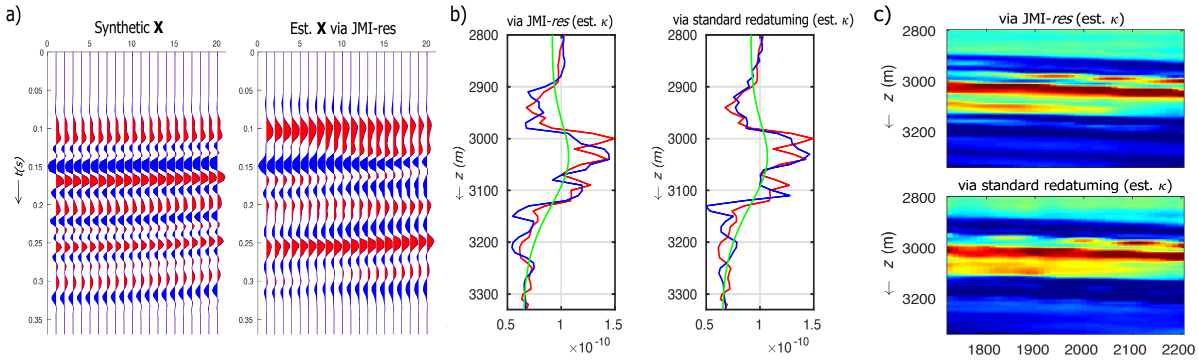

Figure 4: *a) Comparison of the syntheic data via well measurements and the JMI-res estimated impulse responses (**X**) in the $\tau - p$ domain. b) Comparison of κ_{est} at the well location. Red, blue and green corresponds to true, estimated and background values. c) Comparison of 2D κ_{est} section for all locations.*

can be substantial due to recovered transmission losses. Moreover, this approach helps us to avoid using computationally intensive elastic-FWI for the whole subsurface, but only requires requires a local FWI applied at the reservoir level.

Acknowledgements

We would like to thank the TGS for providing the dataset and permission to publish the results. The first author also thanks the Delphi Consortium members for their continuous support.

References

Bednar, J.B. [2005] A brief history of seismic migration. *Geophysics*, **70**(3), 3MJ–20MJ.

Berkhout, A.J. [2014a] Review paper: An outlook on the future seismic imaging, Part I: forward and reverse modelling. *Geophysical Prospecting*, **62**(5), 911–930.

Berkhout, A.J. [2014b] Review paper: An outlook on the future seismic imaging, Part III: Joint Migration Inversion. *Geophysical Prospecting*, **62**(5), 950–971.

Beryhill, J.R. [1984] Wave-equation datuming before stack. *Geophysics*, **49**, 2064–2066.

Davydenko, M. and Verschuur, D.J. [2017] Full-wavefield migration: using surface and internal multiples in imaging. *Geophysical Prospecting*, **65**(1), 7–21.

Garg, A. and Verschuur, D.J. [2016] Reservoir impulse response estimation using Joint Migration Inversion. *78th EAGE Conference & Exhibition*, Extended abstracts, Th SRS1 12.

Garg, A. and Verschuur, D.J. [2017] Elastic reflectivity preserving full waveform inversion. *87th Annual International Meeting*, SEG, Extended abstracts, 5561–5566.

Garg, A. and Verschuur, D.J. [2018] Reservoir elastic parameters estimation from surface seismic data using JMI-res: a full-wavefield approach. *80th EAGE Conference & Exhibition*, Extended abstracts, Tu D04.

Gisolf, A. and van der Berg, P.M. [2012] Target-oriented elastic full wave form inversion. *74th EAGE Conference & Exhibition*, Extended abstracts, P194.

Hobro, J.W.D., Chapman, C.H. and Robertsson, J.O.A. [2014] A method for correcting acoustic finite-difference amplitudes for elastic effects. *Geophysics*, **79**(4), T243–T255.

Russell, B.H. [2014] Prestack seismic amplitude analysis: An integrated overview. *Interpretation*, **2**(2), SC19–SC36.

Schuster, G.T. and Zhou, M. [2006] A theoretical overview of model-based and correlation-based redatuming methods. *Geophysics*, **71**, SI103–SI110.

Staal, X.R. [2015] *Combined imaging and velocity estimation by Joint Migration Inversion*. Ph.D. thesis, Delft University of Technology.

Virieux, J. and Operto, S. [2009] An overview of full-waveform inversion in exploration geophysics. *Geophysics*, **74**(6), WCC1–WCC26.